Beamforming via large and dense antenna arrays above a clutter

Alrabadi, Osama; Tsakalaki, Elpiniki; Huang, Howard; Pedersen, Gert Frølund

Published in:
I E E E Journal on Selected Areas in Communications

DOI (link to publication from Publisher):
10.1109/JSAC.2013.130218

Publication date:
2013

Document Version
Early version, also known as pre-print

Beamforming via Large and Dense Antenna Arrays above a Clutter

Osama N. Alrabadi, *Member, IEEE,* Elpiniki Tsakalaki, *Member, IEEE,* Howard Huang, *Senior Member, IEEE* and Gert F. Pedersen

***Abstract*— The paper sheds light on the beamforming (BF) performance of large (potentially unconstrained in size) as well as dense (but physically constrained in size) antenna arrays when equipped with arbitrarily many elements. Two operational modes are investigated: Single-layer BF and multi-layer BF. In the first mode, a realistic BF criterion namely the average BF gain is revisited and employed to understand the far-field and the near-field effects on the BF performance of large-scale antennas above a clutter. The diminishing throughput returns in a single-layer BF mode versus the number of antennas necessitate multi-layering. In the multi-layer BF mode, the RF coverage is divided into a number of directive non-overlapping sector-beams in a deterministic manner within a multi-user multi-input multi-output (MIMO) system. The optimal number of layers that maximizes the user's sum-rate given a constrained antenna array is found as a compromise between the multiplexing gain (associated with the number of sector-beams) and the inter-beam interference, represented by the side lobe level (SLL).**

***Index Terms*— Beamforming, Capacity, Clustering channels, EM Coupling, MIMO, Large Arrays, High Order Sectorization.**

I. Introduction

MIMO is a technology that enables multiple parallel data streams to be communicated by equipping the transmitter and the receiver with multiple antennas, without sacrificing extra bandwidth or transmit power. Thanks to scattering environments that make the separation of the transmitted mixture of signals possible by decoding their unique spatial signatures, the data rate achieved by each individual antenna can be added up so that the multiple antennas act as a data rate multiplier [1] [2]. Such scattering environments may exist in indoor propagation scenarios where signal rays (multipaths) are organized into clusters with wide enough angle spread [3]. However, this is not true when considering a base-station (BS) on top of a clutter as the multipath concentration seen by a BS in a rural area is only within 2° and within $5^\circ - 7^\circ$ in urban environments [4]. Based on this, observing independent fading channels at the BS dictates the need for an interelement spacing of several wavelengths (almost ten times the carrier wavelength), leading to impractically large array architectures. The problem of large arrays can be mitigated by deploying collocated polarized antennas [5], or by using parasitic antennas [6], i.e., by employing angular rather than space diversity. However, having the antenna elements decorrelated (be it by distance, polarization or angle) degrades the BF potential of such antenna arrays as grating lobes, i.e., multiple main lobes in the array far-field start to appear. An alternative candidate to diversity MIMO systems is to employ BF MIMO systems where the BS is equipped with a set of correlated antenna elements (almost of half a wavelength spacing) leading to a powerful BF system. The motivation behind such BF communication systems is the fact that the free-space BF gain (which is the highest possible BF gain in a sector-beam) is almost maintained in low angular spread channels [7].

The idea of equipping the BS with BF antennas is scaled up within the 'massive MIMO' concept, which proposes to equip the BS with a huge number of antenna elements [8]. Theoretical results promise unprecedented capacity gains, RF frontends complexity reduction as well as remarkable energy savings [9]. The optimal signal precoding in the limiting conditions is found to be matched filtering. From signal space point of view, matched filtering in low angle spread channels together with a massive array shapes pencil beams directing toward the users' clusters. Massive MIMO is mainly proposed for time division duplex (TDD) systems as the downlink BF weights are estimated from the uplink channel. In this paper, unlike the free-space analysis in [10], we conduct a comprehensive analysis regarding the BF performance of arrays equipped with massive number of antennas, including both the far-field scattering environment, i.e., the distribution of the scatterers in the channel, as well as the near-field environment, i.e., the array electromagnetic (EM) coupling and the power reflections due to impedance mismatch. The far-field analysis is simplified by obtaining the diffused sector-beam as a circular convolution of the free-space sector-beam with the channel angular power spectrum (APS). A proper BF criterion is proposed and utilized to evaluate the BF potential of different array topologies under different propagation conditions. On the other hand, the analysis of the near-field is made tractable by replacing the conventional array steering vector with the vector of the active element responses, thus taking into account the EM coupling with the neighboring antenna elements and the coupling with the chassis of the radome. Regarding the TDD mode of operation, simulation results show that the significance of the full channel state information (CSI) at the transmit BS is small when

Paper received February 1, 2012; revised June 15, 2012. This paper is published in part in the Loughborough Antennas and Propagation Conference (LAPC) 2012.

Osama N. Alrabadi is with the Antennas, Propagation and Radio Networking (APNet) group, Department of Electronic Systems, Aalborg University, DK-9220 Aalborg, Denmark. (e-mail: ona@es.aau.dk).

Elpiniki Tsakalaki is with the APNet group, Department of Electronic Systems, Aalborg University, DK-9220 Aalborg, Denmark. (e-mail: et@es.aau.dk).

Gert F. Pedersen is with the APNet group, Department of Electronic Systems, Aalborg University, DK-9220 Aalborg, Denmark. (e-mail: gfp@es.aau.dk).

Howard Huang is with Bell Labs, Alcatel Lucent (e-mail: Howard.Huang@alcatel-lucent.com).

Digital Object Identifier XXX/JSAC.2012.XXX.

communicating in narrow clustering environments compared to the mere stochastic knowledge. Consequently, instantaneous channel estimation and pilot contamination requirements can be relaxed. We also analyze the BF potential when densifying a constrained physical area with many antennas. It is found that, in theory, dense arrays can still have a high BF gain while having the simplest matching network. However this is true when considering only the array matching efficiency but is hard to get in practice because of the higher Ohmic losses owed to the strong reactive fields [11].

The paper then shifts the analysis from single-layer BF to multi-layer BF. MIMO in such systems is enabled via beam multiplexing where the users' signals are mapped onto a set of orthogonal sector-beams thus leading to multi-beam / multi-data stream communication. In the baseband domain this is done by multiplying the vector of users' data symbols with a precoding matrix each column of which shapes a sector-beam (in the signal space) toward a different user. The signal space analysis is made tractable by employing a set of circularly symmetric sector-beams (i.e., each precoding vector is a cyclic rotation of the other), illuminating a coverage of uniform users distribution. A multi-layer beamforming is applied onto a circular cylindrical array (measured) prototype thus multiplexing $\mathcal{B}$ directive sector-beams. The optimal number of sector-beams that maximizes the users' sum-rate is found as a trade off between the multiplexing gain and the SLL (under size-constrained arrays).

Notation: In the following, boldface lower-case and upper-case characters denote vectors and matrices, respectively. The operators $(\cdot)^*$, $(\cdot)^{\mathrm{T}}$, $(\cdot)^{\mathrm{H}}$, $(\cdot)^{-1}$ designate complex conjugate, transpose, complex conjugate transpose (Hermitian) and matrix inverse operators, respectively. The notation $\mathbf{I}_N$ indicates an identity matrix of size $N \times N$ whereas the notion $\mathcal{CN}(0, \sigma^2)$ refers to circularly symmetric complex Gaussian distribution with zero mean and σ^2 variance. $(\cdot)_{ij}$ returns the $\{i, j\}$ entry of the enclosed matrix and $(\cdot)_i$ returns the ith element of the enclosed vector. $\|\cdot\|$ denotes the Euclidean norm of the enclosed vector and $|\cdot|$ returns the absolute value. $\mathbb{E}\{\cdot\}$ is the expectation operator and $\mathbb{C}$ denotes the set of complex numbers of the specified dimensions. The operators $\in$ and $\sim$ indicate that the (random) variable belongs to a certain set of numbers and to a certain distribution, respectively.

The rest of the paper is divided as follows: Section II describes different antenna array models to be utilized later for BF and throughput analysis. Section III sheds light on single-layer BF systems whereas Section IV extends the analysis to multi-layer BF. Finally, Section V suggests some future work.

II. Array System Models

In this paper we consider different antenna array topologies ranging from a uniform linear array (ULA), a uniform cicular array (UCA) and uniform cylindrical array (UCyA). The most common and most analyzed geometry is the ULA which consists of N antenna elements placed on a straight line. We employ ULA topologies for investigating the BF potential of large arrays by increasing the array elements while fixing the interelement spacing (to a distance at which the EM coupling can be safely assumed negligible), thus the array length keeps increasing (potentially size-unconstrained). The steering vector $\boldsymbol{\alpha}(\varphi) \in \mathbb{C}^{N\times 1}$ of a ULA of N isotropic elements has the Vandermonde structure [12] such that

$$\left(\boldsymbol{\alpha}(\varphi)\right)_n = \exp\left(jn\kappa d\cos(\varphi)\right), \tag{1}$$

where $n \in \{1, \ldots, N-1\}$, d is the interelement spacing in wavelengths, $\kappa = 2\pi/\lambda$ is the wavenumber, λ is the free-space wavelength and φ is the azimuthal angle. From signal precoding point of view, a large number of BF techniques have been taken from digital signal processing to shape far-field patterns with small 3dB power beamwidth a.k.a. half-power beamwidth (HPBW), or low SLL. These techniques perform a type of weighting over the array elements by adopting proper functions, such as Gaussian, Kaiser-Bessel [14] and Blackman windows [15]. Widely adopted synthesis techniques for ULAs are the Dolph-Tschebyscheff [16] and the binomial methods [17], which consider a nonuniform distribution of the excitation amplitudes. Comparing the characteristics of uniform, Tschebyscheff and binomial arrays, it can be observed that the uniform arrays provide the smallest HPBW and the highest SLL while the binomial arrays yield the largest HPBW and the lowest SLL [17]. In particular, a binomial array with interelement spacing lower than or equal to half the carrier wavelength has no side lobes. The HPBW and the SLL of a Tschebyscheff array lie between those of binomial and uniform arrays. Besides, for a given SLL, the Dolph-Tschebyscheff arrays provide the smallest first null beamwidth (FNBW) and, reciprocally, for a given FNBW, the Dolph-Tschebyscheff arrays provide the lowest possible SLL.

Another commonly employed configuration is the UCA [18] in which the elements are regularly arranged on a circular ring. The UCA has significant practical interest and is often adopted in radar and sonar systems as well as in cellular BSs. In this paper we employ the UCA mainly for investigating the BF potential of the array when densified with many antenna elements while fixing the array physical area (size-constrained array). Our choice on the UCA topology is owed to the UCA's high degree of symmetry simplifying the analysis. Therefore, we consider a UCA of radius r and N half-wavelength thin electrical dipoles. For properly calculating the EM coupling, the type of the antenna elements comprising the UCA as well as the elements' terminations need to be specified. All the dipoles are terminated with the characteristic real impedance $\mathcal{Z}_{\mathrm{o}}(\Omega)$ which is the simplest matching technique. Along these lines we should remark that such simple matching is favored to sophisticated decoupling and matching networks (DMN) as the complexity of the DMN grows significantly when dealing with more than three antennas [19]. Moreover, the insertion losses introduced by such complex networks are larger than the matching efficiency gains that can be recovered [20]. Finally, the use of DMN, in general, reduces the operative bandwidth of the array [21]; this needs to be taken into account, especially for wideband communication systems.

As stated before, the UCA will be employed to investigate the BF potential of size-constrained arrays, thus the active element response rather than the ideal response should be considered (because of the non negligible effect of the EM coupling). The active element response is the radiation pattern

obtained when exciting the corresponding antenna element with a unit excitation voltage signal while terminating the other antenna elements with their corresponding matching impedances [22]. Consequently, the active element response takes into account the EM coupling with the neighboring antenna elements and the coupling with the chassis of the radome. The active element response of the first element can be expressed as

$$\mathcal{G}_1(\varphi) := \boldsymbol{\alpha}^{\mathrm{T}}(\varphi)(\boldsymbol{\mathcal{Z}}_{\mathrm{T}} + \mathcal{Z}_{\mathrm{o}}\mathbf{I}_N)^{-1}\mathbf{u}_1, \tag{2}$$

where $\boldsymbol{\alpha}(\varphi) \in \mathbb{C}^{N\times 1}$ is the array steering vector under no EM coupling, defined from the array topology as

$$\left(\boldsymbol{\alpha}(\varphi)\right)_n = \exp\left(-j\kappa r\cos(\varphi - (n-1)\frac{2\pi}{N})\right), \tag{3}$$

where $n \in \{1,\ldots,N-1\}$. In (2), $\boldsymbol{\mathcal{Z}}_{\mathrm{T}}$ is the mutual impedance matrix calculated using the analytical expressions in the Appendix and $\mathbf{u}_1$ is a selection vector given by

$$\mathbf{u}_1 = [1 \underbrace{0\ 0\ \ldots\ 0}_{N-1}]^{\mathrm{T}}. \tag{4}$$

In general, $\mathbf{u}_k$ is defined as a vector of all zeros except a unity at the kth position. The active element response of the kth element is given by

$$\left(\boldsymbol{\mathcal{G}}(\varphi)\right)_k = \mathcal{G}_k(\varphi) = \mathcal{G}_1\left(\varphi - \frac{2\pi}{N}(k-1)\right)\exp\left(-j\kappa r\cos\left(\varphi - \frac{2\pi}{N}(k-1)\right)\right) \tag{5}$$

i.e., the kth element response is a rotated and phase-shifted version of the first element response $\mathcal{G}_1(\varphi)$. On the other hand, the input impedance seen by all elements is equal (by the array symmetry). The input impedance can be written in a compact form as

$$\mathcal{Z}_{\mathrm{in}} = \frac{\mathbf{u}_1^{\mathrm{T}}\boldsymbol{\mathcal{Z}}_{\mathrm{T}}\left(\boldsymbol{\mathcal{Z}}_{\mathrm{T}} + \mathcal{Z}_{\mathrm{o}}\mathbf{I}_N\right)^{-1}\mathbf{u}_1}{\mathbf{u}_1^{\mathrm{T}}\left(\boldsymbol{\mathcal{Z}}_{\mathrm{T}} + \mathcal{Z}_{\mathrm{o}}\mathbf{I}_N\right)^{-1}\mathbf{u}_1}. \tag{6}$$

The input reflection coefficient is expressed as [25]

$$\Gamma_{\mathrm{in}} = \frac{\mathcal{Z}_{\mathrm{in}} - \mathcal{Z}_{\mathrm{o}}}{\mathcal{Z}_{\mathrm{in}} + \mathcal{Z}_{\mathrm{o}}}, \tag{7}$$

from which the matching efficiency of each element becomes [25]

$$\eta_k = 1 - \Gamma_{\mathrm{in}}\Gamma_{\mathrm{in}}^* \quad \forall\, k. \tag{8}$$

Although ULAs and UCAs are widely adopted geometries based upon a regular and symmetrical design, these configurations are mainly suitable for applications in which the mounting support is able to sustain the structure and particular size or shape constraints are not present. However, in many practical scenarios, the mounting surface is irregular and/or the available space is limited. In these situations the array geometry must be designed to match the particular requirements of the support and so a conformal array is needed. The antenna elements can be disposed on an ellipse, on an arc, or can be placed according to more complex three-dimensional topologies, usually circularly symmetric surfaces, such as cylinders, cones or spheres [26]. We consider a practical array design for BS, namely the UCyA. We study a UCyA prototype (rather than a theoretical model) comprised of a cylindrical radome with a radius $r = 2.17\lambda$. The array is equipped with $N = 24$ vertical column elements spaced by 0.55λ. Each column is comprised of four patch antennas thus a total of 96 patch antennas exist. The array as well as the measured column (active) response are shown in Fig. 1. The rest of the entries of $\boldsymbol{\mathcal{G}}(\varphi)$ are obtained from the same expression (5), i.e., by physical rotation along with phase-shifting.

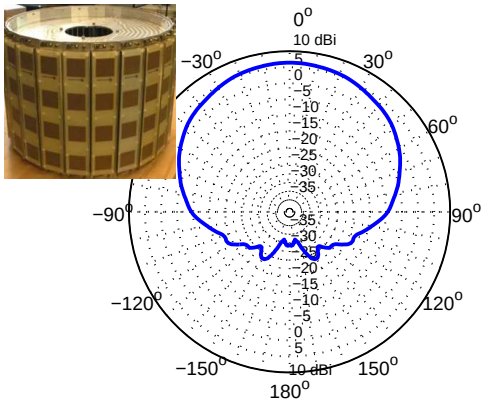

Fig. 1. UCyA Prototype (left) and the array diagram of the measured active element response at 2.45 GHz with a bore-sight gain of 6.4 dBi (right).

III. Single-Layer BF

A. Signal Model

Assume a BS equipped with an array of N antenna elements beaming a complex data symbol x_{T} toward a single antenna user terminal by exciting the antenna elements with the BF vector $\mathbf{w}$ (normalized to a unit power, i.e., $\mathbf{w}^{\mathrm{H}}\mathbf{w} = 1$). Using the Kronecker separability [27], the signal received by the user terminal can be expressed as

$$y = \sqrt{\rho}\mathbf{h}^{\mathrm{H}}\mathbf{w}x_{\mathrm{T}} + n = \sqrt{\rho}\widetilde{\mathbf{h}}^{\mathrm{H}}\mathbf{R}_{\mathrm{T}}^{\frac{1}{2}}\mathbf{w}x_{\mathrm{T}} + n, \tag{9}$$

where $n \sim \mathcal{CN}(0,1)$ is the noise symbol at the receiver side, $\mathbf{h} \in \mathbb{C}^{N\times 1}$ is the complex conjugate of the channel vector between the transmit array and the receive antenna such that $\mathbf{h} \sim \mathcal{CN}(0,\mathbf{R}_{\mathrm{T}})$. $\widetilde{\mathbf{h}} \in \mathbb{C}^{N\times 1}$ is an independent and identically distributed channel vector such that $\widetilde{\mathbf{h}} \sim \mathcal{CN}(0,\mathbf{I}_N)$. The transmit signal-to-noise ratio (SNR) is denoted by ρ whereas $\mathbf{R}_{\mathrm{T}}$ is transmit correlation matrix defined as

$$\mathbf{R}_{\mathrm{T}} := \frac{\mathbb{E}_{\mathbf{h}}\left\{\mathbf{h}\mathbf{h}^{\mathrm{H}}\right\}}{\sqrt{\mathbb{E}_{\mathbf{h}}\left\{\|\mathbf{h}\|_{\mathrm{F}}^2\right\}}}. \tag{10}$$

From a signal space point of view, the transmit correlation

matrix can be alternatively found by obtaining the transmit covariance matrix as

$$\mathbf{R}_{\mathrm{C}} = \oint \boldsymbol{\alpha}(\varphi)\boldsymbol{\alpha}^{\mathrm{H}}(\varphi)\mathcal{A}(\varphi)d\varphi, \tag{11}$$

where $\mathcal{A}(\varphi)$ is the channel APS. From (11) the correlation (normalized covariance) matrix becomes

$$(\mathbf{R}_{\mathrm{T}})_{ij} = \frac{(\mathbf{R}_{\mathrm{C}})_{ij}}{\sqrt{(\mathbf{R}_{\mathrm{C}})_{ii}\,(\mathbf{R}_{\mathrm{C}})_{jj}}} \quad \forall\{i,j\} \in \{1,\ldots,N\}. \tag{12}$$

The fact that the transmit covariance can be either expressed by the expectation of the channel fading vectors' outer product (10) or alternatively by the integration of the array steering vectors' outer product (11) is explained in [28]. The steering vector conventionally represents the responses of antenna elements when each element is alone, i.e., when there is no EM coupling with the other antenna elements or any neighboring objects. However this is not the case in real-life antenna implementations and thus (11) is replaced with

$$\mathbf{R}_{\mathrm{C}} = \oint \boldsymbol{\mathcal{G}}(\varphi)\boldsymbol{\mathcal{G}}^{\mathrm{H}}(\varphi)\mathcal{A}(\varphi)d\varphi, \tag{13}$$

where $\boldsymbol{\mathcal{G}}(\varphi)$ is a column vector formed by stacking the array active element responses. The kth active element response is normalized such that

$$\oint \mathcal{G}_k(\varphi)\mathcal{G}_k^*(\varphi)d\varphi = \eta_k, \tag{14}$$

where η_k is the efficiency of the kth element. In (9), if we set $\mathbf{w}$ to be equal to the eigenvector that corresponds to the maximum eigenvalue of $\mathbf{R}_{\mathrm{T}}$, then the signal model becomes

$$y = \sqrt{\rho}hx_{\mathrm{T}} + n, \tag{15}$$

where the composite channel $\mathbf{h}^{\mathrm{H}}\mathbf{w}$ is replaced by the fading component $h \in \mathbb{C}^{1\times 1}$, $h \sim \mathcal{CN}(0, \lambda_{\max}(\mathbf{R}_{\mathrm{T}}))$ and $\lambda_{\max}(\mathbf{R}_{\mathrm{T}})$ is the maximum eigenvalue of $\mathbf{R}_{\mathrm{T}}$ corresponding to the array beamforming gain or the variance of h. The signal model in (15) can be further written as

$$y = \sqrt{\rho\lambda_{\max}(\mathbf{R}_{\mathrm{T}})}\;\widetilde{h}x_{\mathrm{T}} + n, \tag{16}$$

where $\widetilde{h} \sim \mathcal{CN}(0,1)$.

B. Proper BF Criterion

The normalization in (12) which is found in many text books and research articles, e.g. [29] [30], *does not* reflect the actual BF potential or the directivity of the antenna array as the BF gain $\lambda_{\max}(\mathbf{R}_{\mathrm{T}})$ from (12) is merely connected to the number of the antenna elements. For example, a N-element small-sized as well as a N-element large-sized ULA will both have a free-space BF gain equal of $\lambda_{\max}(\mathbf{R}_{\mathrm{T}}) = N$ based on such normalization. This is indeed not true as we shall explain in the lines. In order to resolve BF gain conflict, we review the concept of the distributed directivity $\mathcal{D}$ which measures the array potential of focusing the power in a certain direction. Assume a free-space sector-beam $\mathcal{G}_{\text{tot}}(\varphi)$ illuminating a cluster of scatterers with an APS of $\mathcal{A}(\varphi)$, such that the cluster center of mass is aligned with the beam bore-sight, then the array directivity $\mathcal{D}$ is defined from [4] as

$$\mathcal{D} := \frac{\oint \mathcal{G}_{\text{tot}}(\varphi)\mathcal{G}_{\text{tot}}^*(\varphi)\mathcal{A}(\varphi)d\varphi}{\frac{1}{2\pi}\oint \mathcal{G}_{\text{tot}}(\varphi)\mathcal{G}_{\text{tot}}^*(\varphi)d\varphi} = \frac{1}{P_{\mathrm{T}}}\oint \mathcal{P}(\varphi)\mathcal{A}(\varphi)d\varphi, \tag{17}$$

where $\mathcal{P}(\varphi) = \mathcal{G}_{\text{tot}}(\varphi)\mathcal{G}_{\text{tot}}^*(\varphi)$ is the *power* sector-beam and P_{T} is the transmit power. Please notice that (17) is a generalization of the free-space directivity obtained by setting $\mathcal{A}(\varphi) = \delta(\varphi - \phi_{\max})$, i.e., zero angle spread channel (Dirac function) in the direction of the maximum power $\phi_{\max}$. Moreover, (17) can be generalized to all angles, thus $\mathcal{D}(\varphi)$ is obtained by the circular convolution of $\mathcal{P}(\varphi)$ with $\mathcal{A}(\varphi)$ thus obtaining

$$\mathcal{D}(\varphi) = \frac{1}{P_{\mathrm{T}}}\oint \mathcal{P}(\phi)\mathcal{A}(\phi - \varphi)d\phi. \tag{18}$$

The distributed directivity is a figure of merit for designing BS antennas [4] analogous to the directivity of point-to-point applications. The better the average match of the sector-beam to the distribution of the scatterers, the better the average gain of the multipath components. The average BF gain $\mathcal{G}_{\text{av}}$ can now be obtained by multiplying the distributed directivity with the array efficiency η_{T}, i.e.,

$$\mathcal{G}_{\text{av}} = \eta_{\mathrm{T}}\mathcal{D}. \tag{19}$$

The free-space sector-beam $\mathcal{G}_{\text{tot}}(\varphi)$ of an array of N antenna elements is generally expressed as

$$\mathcal{G}_{\text{tot}}(\varphi) = \mathbf{w}^{\mathrm{H}}\boldsymbol{\mathcal{G}}(\varphi). \tag{20}$$

By plugging (20) into (17) we get

$$\begin{aligned}\mathcal{D} &= \frac{\oint \left(\mathbf{w}^{\mathrm{H}}\boldsymbol{\mathcal{G}}(\varphi)\right)\left(\mathbf{w}^{\mathrm{H}}\boldsymbol{\mathcal{G}}(\varphi)\right)^{\mathrm{H}}\mathcal{A}(\varphi)d\varphi}{\frac{1}{2\pi}\oint \left(\mathbf{w}^{\mathrm{H}}\boldsymbol{\mathcal{G}}(\varphi)\right)\left(\mathbf{w}^{\mathrm{H}}\boldsymbol{\mathcal{G}}(\varphi)\right)^{\mathrm{H}}d\varphi} \\ &= \frac{\mathbf{w}^{\mathrm{H}}\left(\oint \boldsymbol{\mathcal{G}}(\varphi)\boldsymbol{\mathcal{G}}^{\mathrm{H}}(\varphi)\mathcal{A}(\varphi)d\varphi\right)\mathbf{w}}{\mathbf{w}^{\mathrm{H}}\left(\frac{1}{2\pi}\oint \boldsymbol{\mathcal{G}}(\varphi)\boldsymbol{\mathcal{G}}^{\mathrm{H}}(\varphi)d\varphi\right)\mathbf{w}} = \frac{\mathbf{w}^{\mathrm{H}}\mathbf{R}_{\mathrm{C}}\mathbf{w}}{\mathbf{w}^{\mathrm{H}}\mathbf{R}_{\mathrm{U}}\mathbf{w}}.\end{aligned} \tag{21}$$

From (21), the distributed directivity in a channel of a given APS is maximized when the precoding vector is equal to

$$\mathbf{w}_{\text{opt}} = \mathcal{V}(\mathbf{R}_{\mathrm{C}}, \mathbf{R}_{\mathrm{U}}), \tag{22}$$

where $\mathcal{V}(\cdot)$ is the operator that returns the eigenvector that corresponds to the maximum generalized eigenvalue $\lambda_{\max}(\mathbf{R}_{\mathrm{C}}, \mathbf{R}_{\mathrm{U}})$. In order to highlight the importance of the average BF gain criterion we consider ULAs of N isotropic antennas, spaced by a sufficient interelement spacing such that the EM coupling is safely assumed negligible whereas the elements' efficiencies are set to unity. Fig. 2 shows the broadside sector-beams obtained by driving two ULAs with $\mathbf{w}_{\text{opt}}$ in (22). The sector-beam of the ULA with $d = 0.5$ is

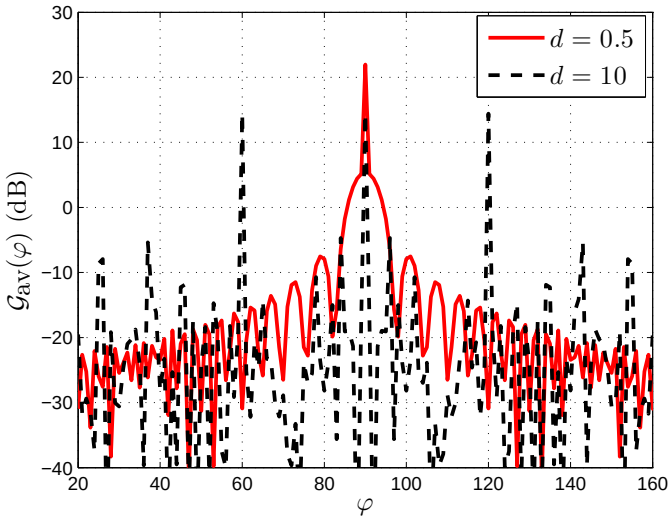

Fig. 2. The sector-beam when exciting with $\mathbf{w}_{\text{opt}}$ in (22) a ULA of 100 isotropic antenna elements for $d = 0.5$ and $d = 10$ spacing.

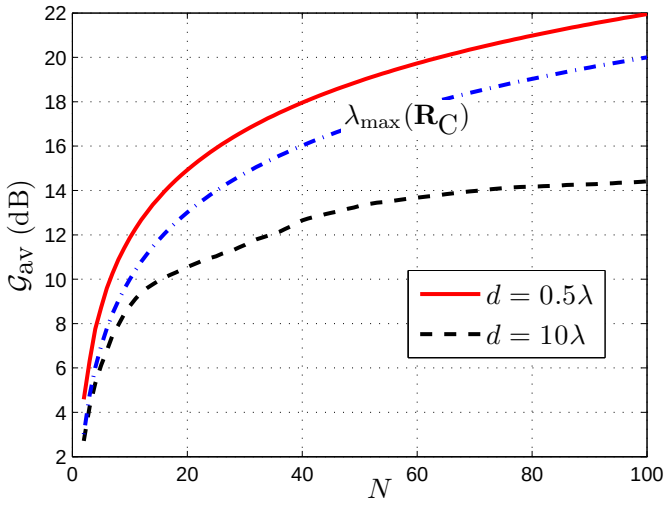

Fig. 3. The average BF gain when exciting with $\mathbf{w}_{\text{opt}}$ in (22) a ULA of 100 isotropic antenna elements for $d = 0.5$ and $d = 10$ spacing.

more directive than the ULA with $d = 10$. This is indeed logical as the antenna elements of the latter array lie out of the correlation distance from each other thus leading to multiple main lobes as illustrated in the same figure. Fig. 3 shows $\mathcal{G}_{\text{av}}(\varphi = \pi/2)$ for both ULAs versus the number of the antenna elements, together with $\lambda_{\max}(\mathbf{R}_{\text{T}})$ for both arrays (coinciding over one another which is not logical). The figure shows that $\lambda_{\max}(\mathbf{R}_{\text{T}})$ may overestimate or underestimate the true BF gain according to the scenario.

Finally, the signal model in (15) can now be accurately replaced with

$$y = \sqrt{\rho \mathcal{G}_{\text{av}}}\ \widetilde{h} x_{\text{T}} + n. \tag{23}$$

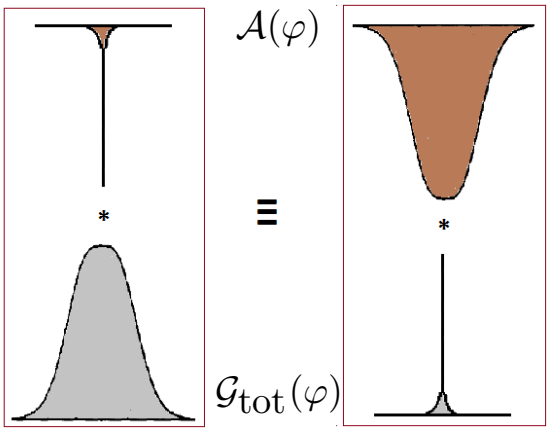

Fig. 4. An illustration of the mutual interaction between the sector-beam and the channel statistics ($*$ indicates circular convolution).

C. Effect of Channel Statistics

In order to understand the interaction between the sector-beam and the channel statistics represented by $\mathcal{A}(\varphi)$ we assume a Gaussian free-space sector-beam with a HPBW of $\sigma_{\mathcal{G}}\sqrt{2\ln 2}$ and zero mean angle, thus according to [4] we get

$$\mathcal{G}_{\text{tot}}(\varphi) := \frac{1}{\sqrt{2\pi}\sigma_{\mathcal{G}}^2} \exp\left(-\frac{\varphi^2}{2\sigma_{\mathcal{G}}^2}\right). \tag{24}$$

We also assume a Gaussian cluster of scatterers with a HPBW of $\sigma_{\mathcal{A}}\sqrt{2\ln 2}$ and zero mean angle, i.e., aligned with the sector-beam, thus

$$\mathcal{A}(\varphi) := \frac{1}{\sqrt{2\pi}\sigma_{\mathcal{A}}^2} \exp\left(-\frac{\varphi^2}{2\sigma_{\mathcal{A}}^2}\right). \tag{25}$$

By convolving (24) with (25) we obtain

$$\mathcal{D}(\varphi) = \frac{1}{P_{\text{T}}\sqrt{2\pi}\left(\sigma_{\mathcal{G}}^2 + \sigma_{\mathcal{A}}^2\right)} \exp\left(-\frac{\varphi^2}{2\left(\sigma_{\mathcal{G}}^2 + \sigma_{\mathcal{A}}^2\right)}\right), \tag{26}$$

i.e., the diffused beam is Gaussian too. The convolution in (26) was performed by first taking the Fourier transform of (24) and (25), multiplying them and then taking the inverse Fourier transform of the product. From (26), if $\sigma_{\mathcal{G}} << \sigma_{\mathcal{A}}$, i.e., the sector-beam is too sharp with respect to the cluster, the resultant diffused beam will have angle spread slightly bigger than the cluster spread. On the other hand, if $\sigma_{\mathcal{G}} >> \sigma_{\mathcal{A}}$ then the free-space sector-beam is almost identical to the diffused beam. Fig. 4 illustrates how a Gaussian beam of certain HPBW, illuminating a nearly zero angular spread cluster is equivalent to a pencil beam illuminating a cluster having the same HPBW of the Gaussian beam.

From (26), the (maximum) array directivity is obtained by setting $\varphi = 0°$, thus we get $\mathcal{D}_{\max} = \mathcal{D}(0) \propto [(\sigma_{\mathcal{B}}^2 + \sigma_{\mathcal{A}}^2)]^{-1}$. Moreover, since the number of antennas N is gen-

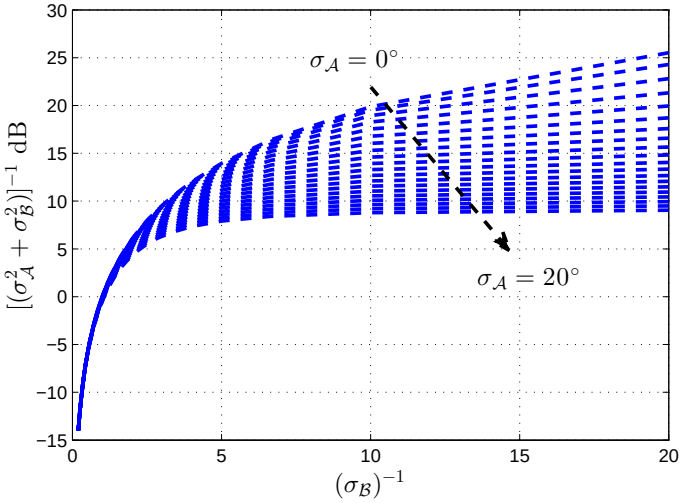

Fig. 5. Maximum distributed directivity $\mathcal{D}(0) \propto [(\sigma_{\mathcal{B}}^2 + \sigma_{\mathcal{A}}^2)]^{-1}$ versus $(\sigma_{\mathcal{B}})^{-1} \propto N$ for different values of $\sigma_{\mathcal{A}}$.

erally proportional to $(\sigma_{\mathcal{B}})^{-1}$ we finally obtain $\mathcal{D}_{\max} \propto \log_{10}\left(\frac{N^2}{1+\sigma_{\mathcal{A}} N^2}\right)$, in dB. From this expression we observe that $\mathcal{D}_{\max} \propto \log_{10}(N)$ in free-space (by setting $\sigma_{\mathcal{A}}$ to zero). On the other hand, $\mathcal{D}_{\max}$ converges to a constant when $(\sigma_{\mathcal{A}})$ increases. In Fig. 5 we plot the maximum directivity versus $(\sigma_{\mathcal{B}})^{-1}$. The same trends are observed in Fig. 6 where a concrete ULA setup is established (with $d = 0.5$) illuminating a cluster of scatterers of angular spread $\sigma_{\mathcal{A}}$. The figure shows that $\mathcal{G}_{\text{av}}$ deteriorates rapidly when illuminating wider and wider clusters (remember that the precoding in (22) is performed according to the channel statistics). On the other hand, Fig. 7 shows free-space sector-beams synthesized by exciting ULAs of 100 and 1000 isotropic elements, 0.5λ spacing with $\mathbf{w}_{\text{opt}}$ in (22). From the figure we drop the following remarks:

- The peak BF gain for both arrays is almost equal when $\sigma_{\mathcal{A}} = 0^\circ$, namely 24.5 dB and 25.5 dB for the 100-element and the 1000-element ULA respectively.
- On the other side, the SLL of the 1000-element ULA is much lower than the SLL of the 100-element ULA. Based on this, wireless systems for which the SLL is vital will benefit by having many antennas, unlike wireless systems that merely benefit from the BF gain. This will be the topic of the next section.
- When the two free-space sector-beams are diffused over a cluster of spread $\sigma_{\mathcal{A}} = 8^\circ$, both sector-beams become identical down to a SLL of -10 dB. Consequently, the 1000-element ULA will provide almost similar performance to the 100-element ULA in channels where the multipath concentration is about 8°. This assures that the optimal number of antennas (to be installed at the BS) beyond which we observe diminishing returns should take the channel statistics into consideration.

D. Effect of Array Efficiency

Till the moment we have been considering potentially unconstrained arrays where the array length grows with the number of the array elements by maintaining the interelement spacing to a minimum of $\lambda/2$ (thus the EM coupling could be safely neglected). In this part we consider physically constrained arrays where the interelement spacing gets smaller when increasing the number of the array elements. The element response when accounting for the EM coupling is given in (2) and (5). On the other hand, the average BF gain according to (19) is the multiplication of the array efficiency[1] and the array distributed directivity $\mathcal{D}$. While $\mathcal{D}$ was shown to be a function of the BF vector $\mathbf{w}$ in (21), it is still not clear how the BF vector affects η_{T}. The transmit array efficiency is in turn the product of the array matching efficiency η_{M} and the array Ohmic efficiency η_{Ω}, i.e., $\eta_{\text{T}} = \eta_{\Omega}\eta_{\text{M}}$. The former is due to the mismatch between the RF source and the load (the antenna) as well as the coupling with the neighboring antennas. The latter is owed to resistive as well as dielectric losses. In this part we assume $\eta_{\Omega} = 1$ which is not true when the quality factor of the array increases. On the other hand, η_{M} in arrays with negligible EM coupling is a mere function of the array terminations and remains constant for all excitations. However this is not true when the array has strong EM coupling among its antenna elements. In this part we overview the way the array efficiency is calculated when simultaneously exciting the elements of an arbitrary array. Given the excitation vector $\mathbf{w}$ the input power is given by $\mathbf{w}^{\text{H}}\mathbf{w}$. Part of the input signal reflects back to the sources, given by $\boldsymbol{\mathcal{S}}_{\text{T}}\mathbf{w}$ where $\boldsymbol{\mathcal{S}}_{\text{T}}$ is the array scattering matrix (normalized to the source impedance). The radiated power is the difference between the incident power and the reflected power while the array efficiency $\eta_{\text{T}} = \eta_{\text{M}}$ is ratio of the radiated power to the input power, i.e.,

$$\begin{aligned} \eta_{\text{T}} &:= \frac{\mathbf{w}^{\text{H}}\mathbf{w} - \mathbf{w}^{\text{H}}\boldsymbol{\mathcal{S}}_{\text{T}}^{\text{H}}\boldsymbol{\mathcal{S}}_{\text{T}}\mathbf{w}}{\mathbf{w}^{\text{H}}\mathbf{w}} \\ &= \frac{\mathbf{w}^{\text{H}}\left(\mathbf{I}_N - \boldsymbol{\mathcal{S}}_{\text{T}}^{\text{H}}\boldsymbol{\mathcal{S}}_{\text{T}}\right)\mathbf{w}}{\mathbf{w}^{\text{H}}\mathbf{w}} = \frac{\mathbf{w}^{\text{H}}\mathbf{T}\mathbf{w}}{\mathbf{w}^{\text{H}}\mathbf{w}}, \end{aligned} \tag{27}$$

where $\mathbf{T} := \mathbf{I}_N - \boldsymbol{\mathcal{S}}_{\text{T}}^{\text{H}}\boldsymbol{\mathcal{S}}_{\text{T}}$ is the radiation matrix. From (27), the maximum efficiency is obtained when the precoding vector

$$\mathbf{w}_{\text{opt}} = \mathcal{V}(\mathbf{T}) \tag{28}$$

is applied, where $\mathcal{V}(\cdot)$ is the operator that returns the eigenvector that corresponds to the maximum eigenvalue $\lambda_{\max}(\mathbf{T})$. Consequently, the precoding vector that maximizes the average BF gain is neither the one that maximizes the array directivity (i.e., the one in (22)) nor the one that maximizes the array efficiency (i.e., the one in (28)), but a compromise in between. Finding the optimal precoding vector that maximizes the average BF gain requires direct search algorithms and gets complicated when the number of the antennas grow. In Fig. 8 we show that the free-space BF gain is quite comparable to the free-space directivity when employing a UCA of N dipoles and $r = \lambda/2$, as modeled in Section II. The dipoles are terminated with $\mathcal{Z}_{\text{o}} = 50\,\Omega$ while the precoding vector is the one in (22). The figure thus shows that *the hit in the*

[1]The array efficiency is different from the elements efficiency η_k. The former is the one obtained when the array elements are excited simultaneously with $\mathbf{w}$ whereas the latter is obtained when the array is excited with $\mathbf{u}_k$.

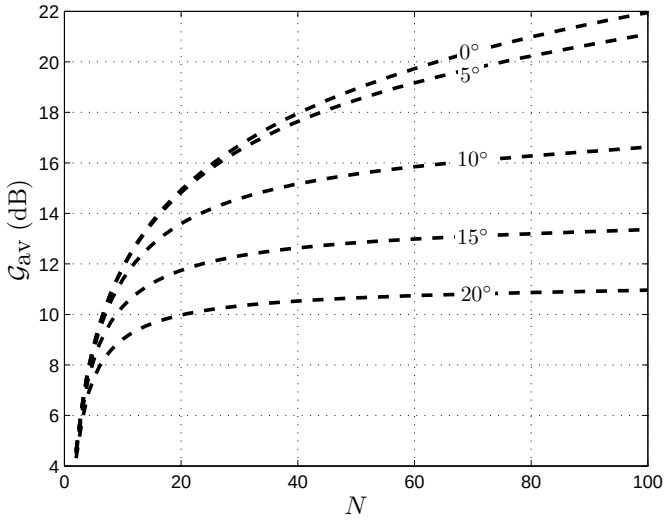

Fig. 6. The average BF gain when exciting with $\mathbf{w}_{\text{opt}}$ in (22) a ULA of N isotropic antenna elements for $d = 0.5$ and $\sigma_{\mathcal{A}} = \{0^\circ,\ 5^\circ,\ 10^\circ,\ 15^\circ,\ 20^\circ\}$.

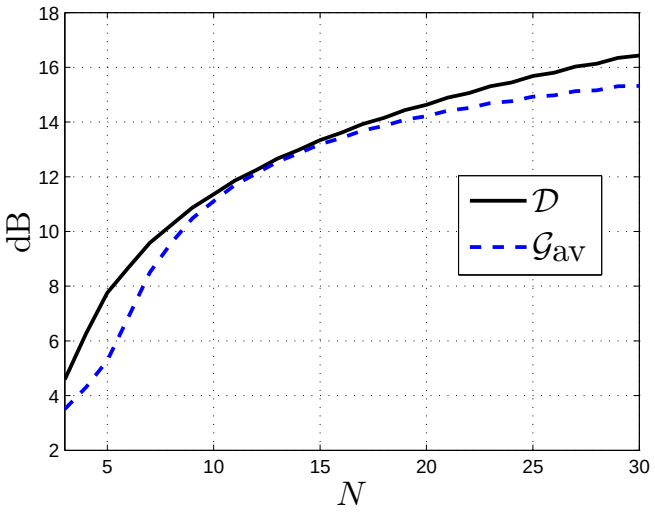

Fig. 8. Free-space directivity and (average) BF gain when exciting with $\mathbf{w}_{\text{opt}}$ in (22) a UCA of N isotropic antenna elements and $r = 0.5$.

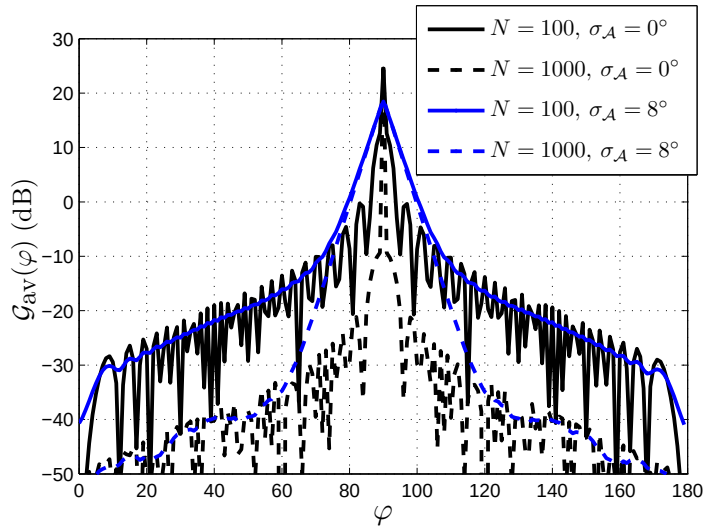

Fig. 7. Free-space and diffused sector-beams when exciting with $\mathbf{w}_{\text{opt}}$ in (22) a ULA of 100 and 1000 isotropic antenna elements whereas $d = 0.5$.

average BF gain owed to the impedance mismatch (matching efficiency) is quite small when driving the array with the excitations that maximize the array directivity. Consequently, maximizing the average BF gain of large-scale antenna arrays can be simply done by maximizing the array directivity using (22) while accepting the (small) hit of the non maximum matching efficiency.

E. Discussion

- In single-layer BF systems the performance is governed by the average BF gain. In non-zero angle spread channels the BF gain tends to saturate beyond a threshold thus further added antennas seem to bring no gain. However, this is not completely true as there could be other hardware and complexity-reduction gains e.g. splitting the power over the antennas relaxes the design of the power amplifiers and RF filters in the transmit RF chain. Moreover, having more antennas immunizes the array against element-branch failures [31].
- From throughput point of view, the logarithmic growth of the capacity with the number of BS antennas is not attractive when operating in a single-layer BF mode. A topology that combines the benefits of diversity as well as BF arrays is illustrated in Fig. 9. The idea is to synthesize a super-array comprised of a set of subarrays. Each subarray *serves as a single directive virtual antenna*. The virtual antennas are decorrelated from each other by distance (could alternatively be by polarization). The subarray preserves most of the BF benefits by having a moderate number of antenna elements within the correlation distance from each other. On the other hand, the super-array preserves the benefits of diversity systems by having the virtual antennas decorrelated. Fig. 10 shows the throughput potential of two subarrays having a total number of antennas N equally divided between the two subarrays, as well as the throughput potential when the N antennas are collocated in one UCA. The RF channel is Rayleigh fading, Laplacian clustering with angle spread of 5° and a mean angle aligned with the broadside axis of symmetry of the two subarrays. The figure shows that 40 collocated antennas provide the same spectral efficiency (or capacity) as 2 (subarrays)$\times$ 4 (antenna/subarray) $= 8$ antennas.
- Last but not least, in order to investigate the (in)significance of full CSI on the throughput potential when transmitting under different channel statistics, we consider a UCA of 20 and 100 dipole elements with $r = 0.5$, illuminating a Laplacian cluster of angle spread $\sigma_{\mathcal{A}}$. Fig. 11 shows the capacity versus the $\sigma_{\mathcal{A}}$ at SNR$= 10$ dB, when partial CSI (denoted by P) is available at the transmit BS, i.e., the UCA is beamforming according to the transmit covariance matrix, and when full CSI (denoted by F) is available, i.e., the UCA is time-reversing the uplink channel [32]. The figure shows that

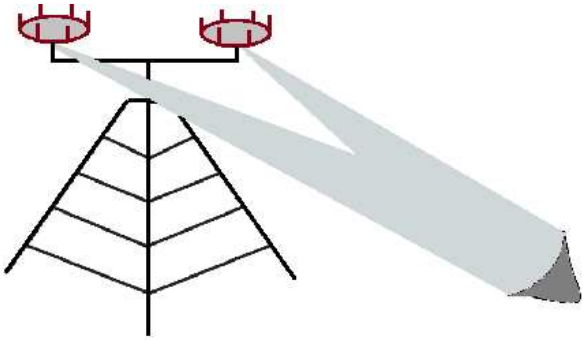

Fig. 9. Super-array topology at a BS above a clutter.

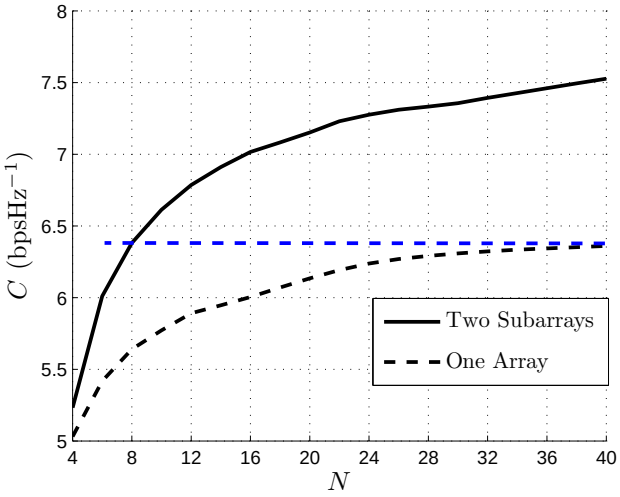

Fig. 10. Capacity performance of a single array of N collocated antennas and a super-array comprised of two subarrays, each subarray has $N/2$ antennas.

the significance of full CSI knowledge decreases as $\sigma_{\mathcal{A}}$ decreases which is an important issue when dealing with channel estimation limits (or pilot contamination issues).

IV. Multi-Layer BF

Till now we have been investigating the BF potential of antenna arrays in a single user scenario thus the term singe-layer BF. However, future wireless systems will allow many users to share the spatial resources within space division multiplexing (SDM). SDM is a technology that allows one BS to serve a number of users in a point-to-multi-point fashion. The key difference between SDM and point-to-point MIMO stems from the independent decoding of the users received signals, thus users' unintended signals are seen as colored noise. The fact that every user knows his own channel but not the others' necessitates careful processing at the BS for minimizing the inter-user interference which otherwise rules out any MIMO multiplexing gain. Generally, this requires a feedback channel from the end users back to the BS which in turn applies a transmit filter like a conventional zero forcing

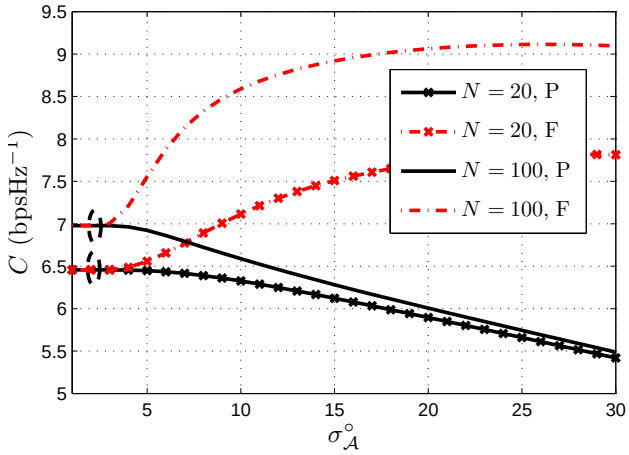

Fig. 11. Capacity performance versus the angle spread of the cluster when partial (P) and full (F) CSI is available at the BS. The performance is shown for two ULAs of 20 and 100 isotropic antenna elements.

precoding matrix. From a beam-space point of view and under *low angle spread channels*, e.g., users' channels seen by a BS on top of a clutter, *the transmit filter maps the users' signals onto a basis of directive beams toward the desired users and nulls toward the interfering ones* i.e., the geometrical and the physical (actual) directions of the channel coincide. A simple SDM technology that utilizes the BF potential of BS arrays is the high order sectorization (HOS) [7] [33]. HOS maps the users' signals onto a *predefined basis of directive sector-beams with low inter-beam interference, regardless* of the users' instantaneous channels. The approach is found practical as it requires the minimum feedback from the users to the BS though some assumptions should be made on the users distribution within the RF coverage. In the following parts we show how the sector-beams can be designed to maximize the system throughput while maintaining full RF azimuthal coverage.

A. Signal Model

We consider a scenario where a set of circularly symmetric sector-beams (see Fig. 12 in [7]) serve a number of users (equal to the number of beams) uniformly distributed within the RF coverage. The precoded signal is given by $\bar{\mathbf{x}} = \mathbf{W}\mathbf{x}$, where $\mathbf{W} \in \mathbb{C}^{N\times\mathcal{B}} = [\mathbf{w}_1\ \mathbf{w}_2\ \ldots \mathbf{w}_{\mathcal{B}}]$ is the precoding matrix, $\mathcal{B}$ is the number of BF layers (sector-beams) and $\mathbf{w}_k$ is the kth precoding vector (cyclic rotation of $\mathbf{w}_1$). $\mathbf{x} = [x_1\ x_2 \ldots x_{\mathcal{B}}]^{\mathrm{T}} \in \mathbb{C}^{\mathcal{B}\times 1}$ is the vector of the complex data symbols to be transmitted. Assuming single antenna users and uniform power distribution across the sector-beams, the signal received by the first user is given by

$$\begin{aligned} y_1 &= \sqrt{\frac{\rho}{\mathcal{B}}}\mathbf{h}_1^{\mathrm{H}}\mathbf{w}_1 x_1 + \sqrt{\frac{\rho}{\mathcal{B}}}\sum_{k=2}^{\mathcal{B}}\mathbf{h}_k^{\mathrm{H}}\mathbf{w}_k x_k + n_1 \\ &= \sqrt{\frac{\rho\mathcal{G}_{\mathrm{av}}(\phi_1)}{\mathcal{B}}}h_1 x_1 + \sqrt{\frac{\rho}{\mathcal{B}}}\sum_{k=2}^{\mathcal{B}}\sqrt{\mathcal{G}_{\mathrm{av}}(\phi_k)}h_k x_k + n_1 \end{aligned} \quad (29)$$

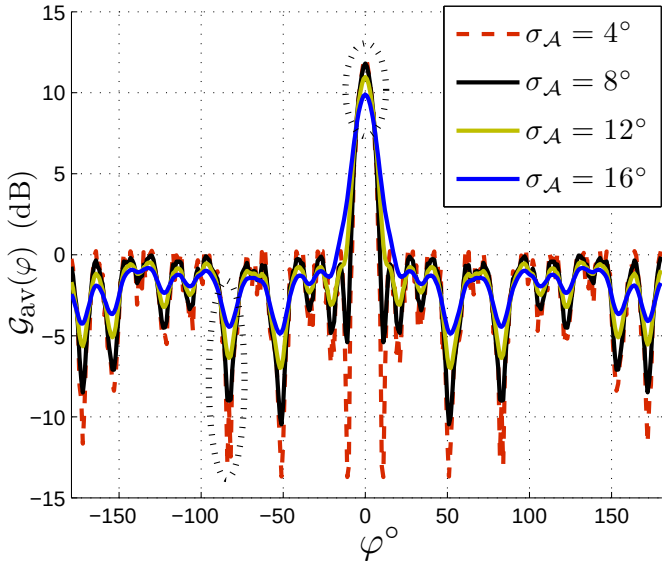

Fig. 12. Effective sector-beam resulting by the convolution the free-space power sector-beam with the channel APS.

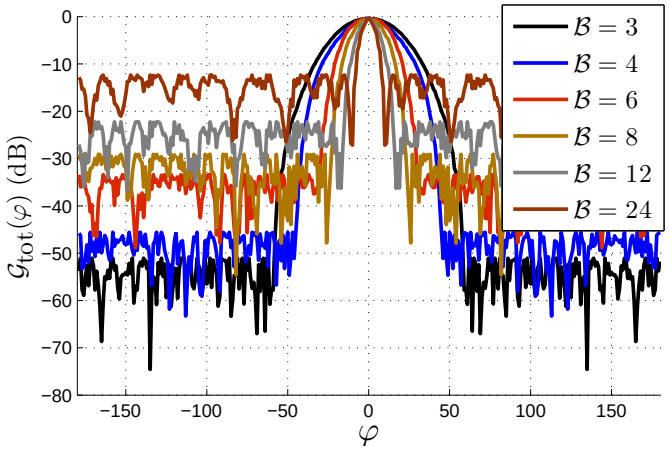

Fig. 13. Free-space sector-beams synthesized using (31) and the UCyA in Fig. 1.

where $h_k \in \mathcal{CN}(0,1)$, $k \in \{1,\ldots,\mathcal{B}\}$ and ϕ_k is the direction of the kth user.

B. Sum-Rate Analysis

Assume every user is immersed in a cluster with a center of mass being uniformly distributed within the angular domain of his sector-beam, then ϕ_j becomes a random variable of uniform distribution within Φ. Assuming every single beam serves one user and by the fact that the users are assumed to be uniformly distributed within the RF coverage, the users' sum-rate will then be equal to the average rate (of one user) scaled by the number of sector-beams as follows:

$$
\begin{aligned}
R_{\Sigma} &= \mathbb{E}_{h,\phi}\left\{\mathcal{B}\log_2\left(1+\text{SINR}(h_1,\phi_1)\right)\right\} && \text{(30a)}\\
&= \mathbb{E}_{h,\phi}\left\{\mathcal{B}\log_2\left(1+\frac{\frac{\rho}{\mathcal{B}}|h_1|^2}{1+\frac{\rho}{\mathcal{B}}\Sigma_{k=2}^{\mathcal{B}}|h_k|^2}\right)\right\} && \text{(30b)}\\
&\leq \mathbb{E}_{h,\phi}\left\{\mathcal{B}\log_2\left(1+\frac{\frac{\rho}{\mathcal{B}}|h_1|^2}{\frac{\rho}{\mathcal{B}}\Sigma_{k=2}^{\mathcal{B}}|h_k|^2}\right)\right\} && \text{(30c)}\\
&\leq \mathbb{E}_{\widetilde{h},\phi}\left\{\mathcal{B}\log_2\left(1+\frac{\mathcal{G}_{\text{av}}(\phi_1)|\widetilde{h}_1|^2}{\ell\Sigma_{k=2}^{\mathcal{B}}|\widetilde{h}_j|^2}\right)\right\} && \text{(30d)}\\
&\leq \mathbb{E}_{\phi}\left\{\mathcal{B}\log_2\left(1+\mathbb{E}_{\widetilde{h}}\left\{\frac{\mathcal{G}_{\text{av}}(\phi_1)|\widetilde{h}_1|^2}{\ell\Sigma_{k=2}^{\mathcal{B}}|\widetilde{h}_j|^2}\right\}\right)\right\} && \text{(30e)}\\
&= \mathbb{E}_{\phi}\left\{\mathcal{B}\log_2\left(1+\frac{\mathcal{G}_{\text{av}}(\phi_1)}{\ell\,(\mathcal{B}-2)}\right)\right\} && \text{(30f)}\\
&\leq \mathcal{B}\log_2\left(1+\frac{\overline{\mathcal{G}}_{\text{av}}}{\ell\,(\mathcal{B}-2)}\right), && \text{(30g)}
\end{aligned}
$$

where SINR is the signal to interference and noise ratio, $\overline{\mathcal{G}}_{\text{av}}$ is the average of $\mathcal{G}_{\text{av}}$ over the random variable ϕ, finally ℓ is the minimum value of $\mathcal{G}_{\text{av}}(\varphi)$. From (30b) to (30c) by the fact that $\log_2(.)$ is a monotonic function. This approximation approaches equality in the high SNR regime. From (30d) to (30e) by the fact that $\ell \leq \mathcal{G}_{\text{av}}(\phi)$. From (30e) to (30f) by the fact that $\frac{|\widetilde{h}_1|^2}{\Sigma_{k=1}^{\mathcal{B}}|\widetilde{h}_j|^2}$ is an F-distribution with a mean $\frac{1}{\mathcal{B}-2}$, Finally from (30f) to (30g) by Jensen's inequality and the concavity of the $\log_2(.)$ function.

C. Sector-Beam Design

Classical filter-design techniques like Prolate [34], Taylor [35], Chebychev [16] etc, can not be directly applied on the proposed UCyA (as the element response may not be factored out) and thus adaptive beamforming techniques are adopted. We set the width of the sector-beam to $\Phi = \frac{2\pi}{\mathcal{B}}$ so that the $\mathcal{B}$ sector-beams cover the full azimuth plane. The distribution of the users is assumed uniform, however other user distributions can be considered resulting in some amplitude tapering within the side-lobes (beyond the scope of this paper). The sector-beam is designed by minimizing the maximum (infinite norm) response within the complementary region of Φ denoted by $\overline{\Phi}$, while maintaining a unit response (with some tolerance τ) at the desired direction ϕ_1 , i.e.,

$$
\begin{aligned}
\underset{(\text{over } \mathbf{w}_1,\, \varphi\in\overline{\Phi})}{\text{minimize}} \quad & \max\left(\mathbf{w}_1^{\text{H}}\boldsymbol{\mathcal{G}}(\varphi)\boldsymbol{\mathcal{G}}^{\text{H}}(\varphi)\mathbf{w}_1\right)\\
\text{subject to} \quad & \text{real}\left(\mathbf{w}_1^{\text{H}}\boldsymbol{\mathcal{G}}(\phi_1)\right) \leq 1+10^{\frac{\tau}{10}}\\
& \text{real}\left(\mathbf{w}_1^{\text{H}}\boldsymbol{\mathcal{G}}(\phi_1)\right) \geq 1-10^{\frac{\tau}{10}} \qquad \text{(31)}
\end{aligned}
$$

(31) is a convex optimization problem that is efficiently handled by the software CVX [36]. The choice of the maximum norm is known to provide the optimal solution by creating side-lobes with equal ripple (thus a constant signal to interference ratio is maintained), while the factor τ ensures the problem not getting over constrained. Having obtained $\mathbf{w}_1$, the circular rotation of $\mathbf{w}_1$ by k taps shifts the direction of the desired response by $\frac{2\pi}{k}$.

- The fact that we optimize the free-space sector-beam in (31) is justified by the slight beam diffusion over

the *narrow* users' clusters. Under a non-zero channel angle spread, the diffused sector-beam will have a smaller BF gain (as explained in Section III) whereas the deep nulls observed in the free-space sector-beam are smeared. Fig. 12 illustrates this by showing the angular convolution of a free-space sector-beam (obtained using (31) and the UCyA in Fig. 1), with a Laplacian APS having angle spread of $4^\circ, 8^\circ, 12^\circ$.

- In order to investigate the tightness of (30g) with respect to (30a), we consider the UCyA in Fig. 1 and optimize its sector-beam using (31). The rest $\mathcal{B}-1$ precoding vectors are obtained by cyclic rotations of $\mathbf{w}_1$ by $\mathcal{B} \in \{3,4,6,8,12,24\}$ rotations. Fig. 15 shows the sum-rate for SNRs of 10, 20 and 30 dB as well as sum-rate upperbound. Although (30g) is somehow loose even at high SNRs, it still provides some useful insights by preserving the same trend of (30a).
- In case the antenna system is constrained, e.g., by size or the number of the antenna elements, then the minimum of the side-lobe level ℓ increases by decreasing Φ, or increasing the number of sector-beams (fundamental trade off [37] as shown in Fig. 13), leading to sum-rate deterioration beyond a threshold number of sector-beams.
- As $\overline{\mathcal{G}}_{\text{av}}$ decreases by increasing the channel spread, the sum-rate consequently degrades as shown in Fig. 14. Notice that in case the channel angle spread becomes relatively wide (e.g. indoor access point surrounded by many scatterers), the multi sector-beams have no multiplexing gain anymore (above a single sector-beam) as the inter-beam interference of the diffused sector-beams becomes intolerable.
- If the ratio $\overline{\mathcal{G}}_{\text{av}}/\ell$ is made independent of the number of beams, for example by keep increasing the array size and the number of the antenna elements (unconstrained antenna system), then the sum-rate upperbound converges asymptotically to $\overline{\mathcal{G}}_{\text{av}}/(\ell \ln(2))$. Thus, the higher the ratio $\overline{\mathcal{G}}_{\text{av}}/\ell$, the higher the system capacity.

Based on the aforementioned remarks, HOS provides considerable performance gains in channels with low angle spread, making such a technique a viable candidate for outdoor cellular systems where feedback is costly and the narrow concentration of multipath is satisfied.

V. Future Work

In the future, we aim at conducting some channel measurement campaigns using both large as well as dense antenna arrays, for better understanding the interaction of the complex RF propagation channel with large-scale antenna systems. An example of the antenna arrays we intend to investigate is the uniform rectangular array shown in Fig. 16, comprised of 64 short monopoles above a small finite a ground operating at $5-6$ GHz. Moreover, since the explosion in the antenna dimension may lead to implosion in the RF hardware dimension, an important issue that we will address is the implementation of reduced-complexity BF-MIMO system architectures. In Fig. 17 we propose a hybrid analogue/digital 2-layers BF system. In such systems, the number of the RF chains scales with $\mathcal{B}$ rather than N. However, each antenna

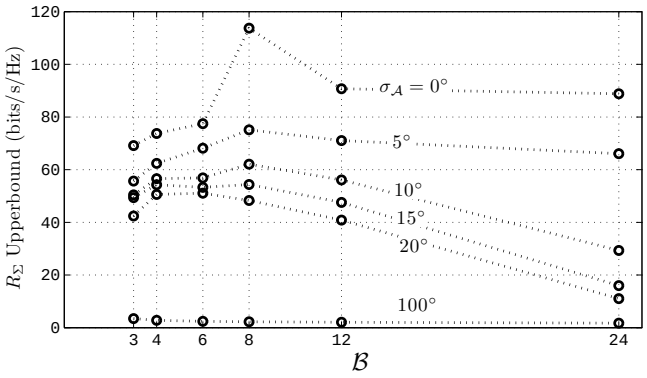

Fig. 14. Users' sum-rate upperbound versus the number of sector-beams at different channel angle spreads. The channel APS is assumed Laplacian with a mean angle that is uniformly distributed within $\frac{2\pi}{\mathcal{B}}$.

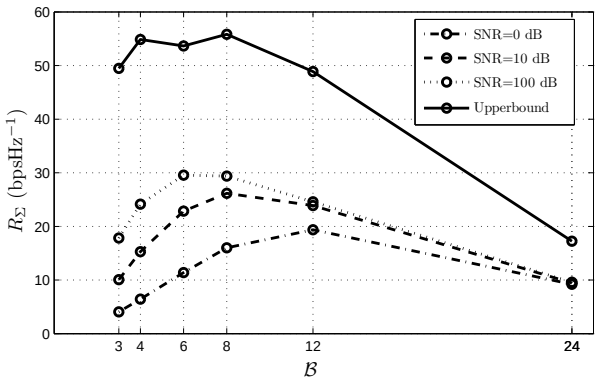

Fig. 15. Users' sum-rate and its upperbound versus the number of sector-beams at different SNRs. The channel APS is assumed Laplacian with a spread of 20° and a mean angle that is uniformly distributed within $\frac{2\pi}{\mathcal{B}}$.

in such architecture is connected to $\mathcal{B}$ paths of analogue gain controllers and phase-shifters. The RF complexity can be further simplified exploiting the concept of HOS where deterministic multi-layer BF approach requires static phase-shifters and gain controls (i.e. static BF network).

Appendix

An approached expression of the dipoles self-impedance is given by the impedance of an n wavelength long isolated dipole [23]:

$$\{\boldsymbol{\mathcal{Z}}_{\text{T}}\}_{ii} = 30\left[\ln(2\pi n\gamma) - \text{CI}(2\pi n) + j\text{SI}(2\pi n)\right], \quad (32)$$

where γ is the Euler constant ($\gamma = 0.5772156649...$) and SI and CI are the sine and cosine integral functions defined as follows

$$\begin{aligned} \text{SI}(z) &= \int_0^z \frac{\sin(t)}{t}dt \\ \text{CI}(z) &= \int_\infty^z \frac{\cos(t)}{t}dt = \gamma + \ln z + \int_0^z \frac{\cos(t)-1}{t}dt\,. \end{aligned} \quad (33)$$

The coupling-impedance terms $\{\boldsymbol{\mathcal{Z}}_{\text{T}}\}_{ij} = \mathcal{R}_{ij} + j\mathcal{X}_{ij},\ i \neq j$

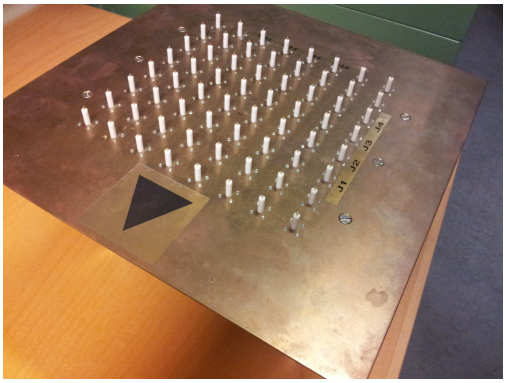

Fig. 16. An array of 64 monopoles above a finite ground, operating at $5-6$ GHz.

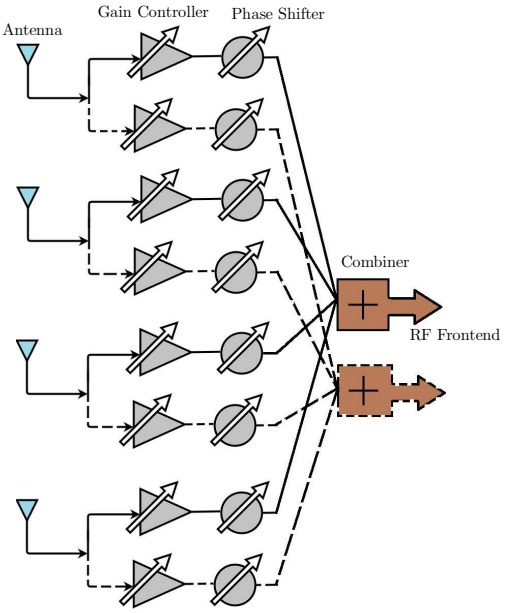

Fig. 17. Hybrid analogue-digital two-layers BF system.

are calculated using the induced electromotive force method [24]

$$\begin{aligned} \mathcal{R}_{ij} &= +\frac{\eta_{\mathrm{f}}}{4\pi}\left[2\mathrm{CI}\left(u_0\right)-\mathrm{CI}\left(u_1\right)-\mathrm{CI}\left(u_2\right)\right], \\ \mathcal{X}_{ij} &= -\frac{\eta_{\mathrm{f}}}{4\pi}\left[2\mathrm{SI}\left(u_0\right)-\mathrm{SI}\left(u_1\right)-\mathrm{SI}\left(u_2\right)\right], \end{aligned} \tag{34}$$

where $u_0 = \kappa d$, $u_1 = \kappa\left(\sqrt{d_{ij}^2+L^2}+L\right)$, $u_2 = \kappa\left(\sqrt{d_{ij}^2+L^2}-L\right)$, $\eta_{\mathrm{f}} = 120\pi$ is the free-space impedance, d_{ij} is the spacing between the ith and the jth adjacent dipoles and $L = \lambda/2$ is the dipole length.

REFERENCES

[1] G. J. Foschini and M. J. Gans,"Limits of wireless communication in a fading environment when using multiple antennas," *Wireless Personal Comm.*, . 6, pp. 311-335, 1998.

[2] I. E. Telatar, "Capacity of multi-antenna Gaussian channels," *European Transactions on Telecommunications*, pp. 585-595, Nov. 1999.

[3] M. Steinbauer, A. F. Molisch and E. Bonek, "The double directional radio channel," *IEEE Ant. and Prop. Mag.*, vol. 43, no. 4, pp. 51-63, 2001.

[4] J. B. Andersen and R. Vaughan, "Channels, Propagation and Antennas for Mobile Communication," 2003.

[5] Y. Ebine, T. Takahashi, and Y. Yamada, "Study of vertical space diversity for land mobile radio," *Electronics and Communications in Japan*, vol.74 no.10 pp. 68-76 , 1991.

[6] R. Vaughan, "Switched Parasitic Elements for Antenna Diversity," *IEEE Trans. on Ant. and Prop.*, vol.47, No.2, Feb-1999.

[7] H. Huang, M. Trivellato, A. Hottinen, M. Shafi, P. Smith, R. Valenzuela, "Increasing downlink cellular throughput with limited network MIMO coordination," *IEEE Trans. on Wireless Comm.*, vol. 8, no. 6 , pp. 2983 - 2989, 2009.

[8] T. L. Marzetta, "Noncooperative cellular wireless with unlimited numbers of base station antennas," *IEEE Trans. Wireless Comm.*, vol. 9, no. 11, pp. 35903600, Nov. 2010.

[9] F. Rusek, D. Persson, B. K. Lau, E. G. Larsson, T. L. Marzetta, O. Edfors, F. Tufvesson, "Scaling up MIMO: Opportunities and Challenges with Very Large Arrays," Accepted at the *IEEE Signal Proc. Mag.*, Oct. 2011.

[10] R. S. Elliott, "Beamwidth and Directivity of Large Scanning Arrays," *Microwave Journal*, Dec. 1963, p.53, and Jan. 1964, p.74.

[11] R. P. Haviland, "Supergain Antennas: Possibilities and Problems," *IEEE Ant. and Prop. Mag.*, vol. 37, no.4, August 1995.

[12] H. Bach and J. E. Hansen, "Uniformly Spaced Arrays," *in Ref. [13], part 1*.

[13] R. E. Collin and F. J. Zucker, eds., "Antenna Theory, parts 1 and 2," *McGraw-Hill*, New York, 1969.

[14] J. F. Kaiser, "Nonrecursive Digital Filter Design Using the Io-Sinh Window Function," *Proc. 1974 IEEE Int. Symp. on Circuits and Systems, p.20, (1974)*, and reprinted in *Selected Papers in Digital Signal Processing, II, edited by the Digital Signal Processing Committee and IEEE ASSP, IEEE Press, New York*, 1976, p.123.

[15] F. Gross, "Smart Antennas for Wireless Communications with Matlab," NewYork, McGraw-Hill, 2005.

[16] C. L. Dolph, "A Current Distribution for Broadside Arrays Which Optimizes the Relationship Between Beam Width and Side-Lobe Level," *Proc. IRE*, 34, 335 (1946).

[17] C. A. Balanis, "Antenna Theory: Analysis and Design," *New York John Wiley and Sons*, 1997.

[18] P. N. Fletcher and P. Darwood, "Beamforming for circular and semi-circular array antenna for low-cost wireless LAN data communication systems," *IEEE Proc. in Micro. and Ant. Prop.*, vol. 145, no. 2, 1998, pp. 153-158.

[19] J. Weber, C. Volmer, K. Blau, R. Stephan, and M. A. Hein, "Miniaturized antenna arrays using decoupling networks with realistic elements," *IEEE Trans. Microwave Theory Tech.*, vol.54, no.6, pp.2733-2740, June 2006.

[20] C. Volmer, J. Weber, R. Stephan, K. Blau and M. A. Hein, "An Eigen-Analysis of Compact Antenna Arrays and Its Application to Port Decoupling.," *IEEE Trans. on Ant. and Prop.*, vol. 56, no. 2, Feb. 2008.

[21] B. K. Lau, J. B. Andersen, G. Kristensson, A. F. Molish, "Impact of matching network on bandwidth of compact antenna arrays" *IEEE Trans. Ant. Prop.*, 2006, 54, 11, 3225-3238.

[22] D. M. Pozar, "The active element pattern," *IEEE Trans. on Ant. and Prop.*, vol. 42, no.8, pp. 1176 - 1178, August 2002.

[23] R. F. Harrington, "Reactively controlled directive arrays," *IEEE Trans. Antennas Propag.*, vol. 26, no. 3, pp. 390395, May 1978.

[24] J. D. Kraus and R. J. Markhefka, "Antenna for All Applications," 3rd ed. Upper Saddle River, NJ: McGraw Hill, 2002.

[25] S. J. Orphanides, "Electromagnetic waves and antennas," Rutgers Univ., 2008.

[26] T. Haruyama, N. Kojima, I. Chiba, Y. Oh-Hashi, N. Orime and T. Katagi,"Conformal Array Antenna with Digital Beam Forming Network," *IEEE Ant. and Prop. Society Intern. Symp. (APS)*, vol. 2, pp. 982985, Jun. 1989.

[27] D. S. Shiu, G. J. Foschini, M. J. Gans, and J. M. Kahn, "Fading correlation and its effect on the capacity of multielement antenna systems, IEEE Trans. Comm., vol. 48, no. 3, pp. 502-513, Mar. 2000.

[28] T. S. Pollock, T. D. Abhayapala, R. A. Kennedy,"Introducing 'space' into space-time MIMO capacity calculations: a new closed form upper bound," *10th Intern. Conf. on Telecomm.*, vol. 2, pp. 1536 - 1541, 2003.

[29] M. A. Jensen and J. W. Wallace, "A review of antennas and propagation for MIMO wireless communications," *IEEE Trans. Ant. Prop.*, vol. 52, pp. 2810-2824, Nov. 2004.

[30] C. Oestges and B. Clerckx,“MIMO Wireless Communication, From Real-World Propagation to Space-Time Code Design,” pages 227-230, First Edition, 2007.
[31] E. P. Tsakalaki, L. A. M. R. de Temino, T. Haapala, J. L. Roman and M. A. Arauzo, “Deterministic beamforming for enhanced vertical sectorization and array pattern compensation,” *the 6th European Conference on Antennas and Propagation, EuCAP 2012*, pp. 2789 - 2793, Prague, Czech Republic 2012.
[32] H. T. Nguyen, J. B. Andersen, G. F. Pedersen, P. Kyritsi and P. C. F. Eggers, “Time Reversal: A Measurement-Based Investigation,” *IEEE Trans. on Wireless Comm.* vol. 5, no. 8, Aug. 2006.
[33] H. Howard, O. N. Alrabadi, J. Daly, D. Samardzija, C. Tran, R. Valenzuela and S. Walker, “Increasing throughput in cellular networks with higher-order sectorization,”*44th Asilomar Conference on Signals, Systems and Computers (ASILOMAR)*, pp. 630 - 635, April 2011.
[34] A. Papoulis and M. S. Bertram, “Digital Filtering and Prolate Functions, IEEE Trans. Circuit Th.,” *CT-19*, 674 (1972).
[35] T. T. Taylor, “Design of Line-Source Antennas for Narrow Beamwidth and Low Side Lobes,” *IRE Trans. Ant. Prop.*, AP-3, 16 (1955).
[36] M. Grant and S. Boyd,“Matlab Software for Disciplined Convex Programming,” version 1.21, April 2011, *http://stanford.edu/ boyd/cvx*.
[37] R. J. Stegen, “The Gain-Beamwidth Product of an Antenna,” *IEEE Trans. Ant. Prop.*, AP-12, 505 (1964).

Osama N. Alrabadi (S’08–M’11) is an industrial postdoctoral fellow at the Antennas, Propagation and radio Networking (APNet) group, department of Electronic Systems, Aalborg University, Denmark. He was born in 1979 in Jordan, where he received the Diploma of Electrical Engineering from the University of Jordan in 2002. He received the M.Sc. in Information and Telecommunications from Athens Information Technology, Greece in 2007 with the highest honor, and the Ph.D. degree from the Aalborg University in 2011. In summer 2010, he was an intern at Bell Laboratories (Alcatel-Lucent), Holmdel, New Jersey, where developed beamforming techniques for cellular networks. Currently he is working on the ”Smart Antenna Frontend (SAFE)” project, in cooperation with the antenna company Molex, the tuner company Wispry (California, US) and Intel Mobile Communications. His research interests include design and modeling of small antenna arrays, array processing as well as MIMO and cognitive radio transceiver architectures. Dr. Osama N. Alrabadi is a co-author of numerous journal and conference papers and holds several patents. He is an IEEE member and a member of the Jordan Engineering Association since 2002.

Elpiniki Tsakalaki is a postdoctoral fellow at the Antennas, Propagation and radio Networking (APNet) group at the department of Electronic Systems,Aalborg University, Denmark, from where she received her Ph.D. degree in Wireless Communications in 2012. With a scholarship from the Hellenic Federation of Enterprises (SEV), she received in 2009 the M.Sc. in Information Networking from the Information Networking Institute, Carnegie Mellon University, Pittsburgh with the highest honor. In 2008, she received the Diploma in Electrical and Computer Engineering (Dipl.-Ing.) from the National Technical University of Athens, Greece. From 2009 until 2012 she worked in the research project ”Cognitive Radio Oriented Wireless Networks (CROWN)” funded under the FET-Open scheme within the Seventh Framework Programme (FP7) of the European Commission. During the summer of 2011 she was an intern at Nokia Siemens Networks, Madrid, Spain, developing beamforming designs for active base station antenna systems. Currently, she is working on the project ”MIMO wireless communications for closely spaced antennas” granted by the Danish Council for Independent Research, Technology and Production Sciences (FTP). Her research interests are in the combined area of antenna design and signal processing including reconfigurable and compact antenna arrays, diversity and MIMO systems, and cognitive radio communication. She is a member of the IEEE and a member of the Technical Chamber of Greece.

Howard Huang was born in Houston, Texas in 1969. He received a BS in electrical engineering from Rice University in 1991 and a Ph.D. in electrical engineering from Princeton University in 1995. Since then, he has been a researcher at Bell Labs (Alcatel-Lucent) in Holmdel, New Jersey, currently as a Distinguished Member of Technical Staff in the Wireless Communication Theory Department. His interests are in communication theory, multiple antenna (MIMO) techniques, and the system design of wireless networks. He served as a guest editor of two issues of the IEEE Journal of Selected Areas in Communications- one on next-generation MIMO wireless networks and another on cooperative communications in MIMO cellular networks. He has taught at Columbia University and is a co-author of the book MIMO Communication for Cellular Networks (published by Springer 2011). Dr. Huang holds over a dozen patents and is a Senior Member of the IEEE.

Gert Frølund Pedersen was born in 1965, married to Henriette and has 7 children. He received the B.Sc. E. E. degree, with honor, in electrical engineering from College of Technology in Dublin, Ireland, and the M.Sc. E. E. degree and Ph.D. from Aalborg University in 1993 and 2003. He has been with Aalborg University since 1993 where he is now full Professor heading the Antenna, Propagation and Networking LAB with 36 researchers. Further he is also the head of the doctoral school on Wireless Communications with around 100 Ph.D. enrolled students. His research has focused on radio communication for mobile terminals especially small antennas, diversity systems, propagation and biological effects and he has published more than 175 peer reviewed papers and holds 28 patents. He has also worked as consultant for developments of more than 100 antennas for mobile terminals including the first internal antenna for mobile phones in 1994 with lowest SAR, first internal triple-band antenna in 1998 with low SAR and high TRP and TIS, and lately various multi antenna systems rated as the most efficient in the market. He has worked most of the time on joint university and industry projects and has received more than 12 million USD in direct research funding. Latest he is the project leader of the SAFE project with a total budget of 8 million USD investigating tunable front-ends including tunable antennas for the future multiband mobile phones. He has been one of the pioneers in establishing Over-The-Air (OTA) measurement systems. The measurement technique is now well established for mobile terminals with single antennas and he has been chairing the various COST groups (swg2.2 of COST 259, 273, 2100 and currently ICT1004) with liaison to 3GPP for OTA testing of MIMO terminals.